# Delay-induced multistable synchronization of biological oscillators

U. Ernst, K. Pawelzik, and T. Geisel

*Institut für Strömungsforschung und Sonderforschungsbereich 185 "Nichtlineare Dynamik," Bunsenstraße 10,
37073 Göttingen, Germany*

We analyze the dynamics of pulse coupled oscillators depending on strength and delay of the interaction. For two oscillators, we derive return maps for subsequent phase differences, and construct phase diagrams for a broad range of parameters. In-phase synchronization proves stable for inhibitory coupling and unstable for excitatory coupling if the delay is not zero. If the coupling strength is high, additional regimes with marginally stable synchronization are found. Simulations with $N \gg 2$ oscillators reveal a complex dynamics including spontaneous synchronization and desynchronization with excitatory coupling, and multistable phase clustering with inhibitory coupling. We simulate a continuous description of the system for $N \to \infty$ oscillators and demonstrate that these phenomena are independent of the size of the system. Phase clustering is shown to relate to stability and basins of attraction of fixed points in the return map of two oscillators. Our findings are generic in the sense that they qualitatively are robust with respect to modeling details. We demonstrate this using also pulses of finite rise time and the more realistic model by Hodgkin and Huxley which exhibits multistable synchronization as predicted from our analysis as well. [S1063-651X(98)09902-4]

PACS number(s): 87.10.+e, 05.45.+b

## I. INTRODUCTION

Synchronization of coupled oscillators is a quite common and elementary phenomenon in many different disciplines such as physics [1–3], chemistry [4], and biology [5]. In the recent years, this topic has gained increasing attention as synchronous oscillations have been observed in the visual cortex [6,7,50], which were related to Gestalt properties of the stimulus. It has been pointed out that synchronous firing activity may be a part of higher brain functions and a method for integrating distributed information in an abstract representation [8,9]. Besides the question of the functional role of synchronization, the mechanisms that lead to this collective behavior were of central interest.

Abstracting from biophysical details, neurons and other biological oscillators have been modeled as phase oscillators with an instantaneous sinusoidal phase coupling, and collective phenomena such as synchronization have been found [3]. This elementary approach has been somewhat generalized to account for more realistic situations by choosing a different interaction function whose shape was determined by the underlying biophysical model, in the case of neurons, e.g., the Hodgkin-Huxley neuron [10]. The higher Fourier modes of these modified functions are known to give rise to phase clustering of the oscillators [11–14]. Furthermore negative coupling has been shown to be important for synchronization [15–17].

However, two problems arise in this context. Every biological system has to deal with substantial delays that seem, heuristically speaking, to constrain the process of synchronization. Nevertheless, the brain manages this problem and even synchronizes neurons across long distances [18]. Secondly, real neurons do not interact continuously but instead exchange pulses at certain times.

A key work about the origins and mechanisms of synchronization which accounts for the pulselike interaction was the analysis of Mirollo and Strogatz [19]. They proposed a model whose amplitude $f(\Phi)$, in the case of neurons the membrane potential, is a smooth function, which is concave down and depends on the time $\Phi$ since the last activation. A prototype of this system is a leaky integrate-and-fire oscillator,

$$\dot{f} = -c_1 f + c_2 \quad \text{with} \quad c_2 > c_1. \tag{1}$$

If $f$ reaches a threshold, the neuron emits a pulse and $f$ is reset to zero, while all the other oscillators in the network increment their amplitudes by an amount $\epsilon$ (excitatory couplings). These conditions always lead to stable in-phase synchronization of the whole network.

In this paper, we investigate the effects of nonzero delays on such oscillators, and we include also inhibitory couplings. In Secs. II and III, we present a complete mathematical analysis for pairs of two Mirollo-Strogatz-type oscillators for a wide range of delays $\tau$ and coupling strengths $\epsilon$, which necessitates a set of intricate case distinctions. We explicitly construct fire maps and return maps, and reveal the existence and stability of all fixed points. For inhibitory couplings, it turns out that the presence of delays can lead to stable in-phase synchronization. For excitatory couplings, we only get out-of-phase synchronization because in-phase synchronization proves to be not stable. Considering higher coupling strengths, the existence of marginal stable regimes for synchronization is shown. These results are summarized in Sec. IV.

In the numerical part of this paper, beginning with Sec. V, we examine the behavior of populations of $N > 2$ up to $N \to \infty$ neurons, which we have simulated numerically. In addition to our previous results, we observe multistable phase clustering for inhibitory couplings, and the spontaneous emergence and decay of synchronized neuronal clusters with excitatory couplings. In Sec. VI, we derive a continuity equation for the dynamics in the limit of $N \to \infty$ neurons that shows that our results do not depend on the system's size. In order to demonstrate that most of our results do not only rely on abstract pulse-coupled oscillators, but also do apply for
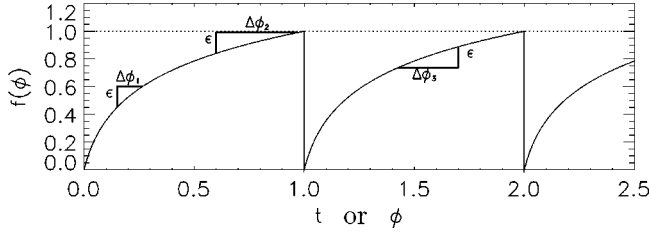
FIG. 1. Function $f(\Phi)$ and the dependence of the phase shift on $\Phi$. With excitatory couplings, an increase of $\epsilon$ in the amplitude $f$ corresponds to a shift of phase that is larger when starting with a larger phase ($\Delta\Phi_2 > \Delta\Phi_1$). A negative phase shift $\Delta\Phi_3$ occurs with inhibitory couplings.

real neurons, we simulate in Sec. VII the more detailed neuron model of Hodgkin and Huxley [20]; and we show that the phenomena found in the simple Mirollo-Strogatz model are preserved in this realistic framework.

## II. MODEL

The network consists of $N$ relaxation oscillators, which are caricatures of real pulse-coupled neurons in biological systems [19]. Each oscillator $i$ may be described by a smooth function $f(\Phi_i)$, which is concave down and monotonically increasing [$f' > 0$, $f'' < 0$, $f(0) = 0$, $f(1) = 1$]. $f$ plays the role of an amplitude (e.g. the membrane potential) and $\Phi_i \in [0,1]$ is a phase, which in the case of vanishing input from other oscillators corresponds to the normalized time elapsed since the last firing of $i$. When $f$ reaches the threshold $f_s := 1$, the oscillator fires and $\Phi_i$ and $f$ are reset to zero. After a time delay $t = \tau$, $\tau \in \, ]0,0.5[$, the spike reaches all the other oscillators (no self-interaction) and raises (excitatory couplings) or lowers (inhibitory couplings) their amplitudes by an amount $\epsilon = \overline{\epsilon}(N-1)^{-1}$, where $\overline{\epsilon}$ denotes the normalized coupling strength ($\overline{\epsilon} \in \, ]0,1]$). The coupling to the oscillators $j$ may be represented equivalently by an increase or decrease in phase $\Delta\Phi_j$ (Fig. 1)

$$\Phi_j + \Delta\Phi_j = f^{-1}(\min[f(\Phi_j) + \epsilon, 1]) := F_+(\Phi_j, \epsilon), \quad (2)$$

$$\Phi_j + \Delta\Phi_j = f^{-1}(\max[f(\Phi_j) - \epsilon, 0]) := F_-(\Phi_j, \epsilon), \quad (3)$$

where Eqs. (2) and (3) refer to excitatory and inhibitory coupling, respectively. We point out that the concavity of $f$ is responsible for the dependence of $\Delta\Phi_j$ on $\Phi_j$, the larger the phase $\Phi_j$, the larger the phase shift $\Delta\Phi_j$ (Fig. 1).

Before we treat a pair of these oscillators in a mathematical analysis, we note some simple properties of the functions $F_-$ and $F_+$ introduced in Eqs. (2) and (3) that we will need in the next paragraph:

$A1$: $F_+(\Phi, \epsilon) > \Phi$ for $\Phi < 1$.

$A2$: $F_-(\Phi, \epsilon) < \Phi$ for $\Phi > 0$.

$A3$: $\quad F_+(c+\Phi, \epsilon) - F_+(c-\Phi, \epsilon) > (c+\Phi) - (c-\Phi) = 2\Phi$ for $c - \Phi > 0$ and $F_+(c+\Phi, \epsilon) < 1$.

$A4$: $0 < F_-(c+\Phi, \epsilon) - F_-(c-\Phi, \epsilon) < (c+\Phi) - (c-\Phi) = 2\Phi$ for $c + \Phi < 1$ and $F_-(c-\Phi, \epsilon) > 0$.

$A5$: $f(\Phi_2) - f(\Phi_1) > f(\Phi_2 + a) - f(\Phi_1 + a)$ if $\Phi_1 < \Phi_2$, $a > 0$, $f' > 0$, and $f'' < 0$.

$A6$: $f(\Phi_1' + a') - f(\Phi_1' - a') > f(\Phi_2' + a') - f(\Phi_2' - a')$ follows directly from $A5$ with $\Phi_1' = \Phi_1 + a/2$, $\Phi_2' = \Phi_2 + a/2$, and $a' = a/2$.

$A7$: $F_+(\Phi_2, \epsilon) - \Phi_2 > F_+(\Phi_1, \epsilon) - \Phi_1$ or, more compact $\Delta\Phi_2 > \Delta\Phi_1$ if $0 < \Phi_1 < \Phi_2$, $f' > 0$, $f'' < 0$, and $F_+(\Phi_2, \epsilon) < 1$.

## III. MATHEMATICAL ANALYSIS

In this section, we will derive phase diagrams that allow one to determine if and how two oscillators synchronize their activities. Speaking in mathematical terms, the repellors and attractors of the dynamics have to be found. We hereby consider a system $S$ of two oscillators $A$ and $B$, both either inhibitorily or excitatorily coupled together with time delay $\tau$. Let us first introduce some basic definitions for our analysis.

To extract the asymptotic behavior of $S$, we keep track of the evolution of the phase difference between the oscillators

$$\Delta\Phi_{i,j}(t) := [1 + \Phi_j(t) - \Phi_i(t)] \quad \mod 1, \quad (4)$$

which is calculated each time $t_{p,i}$ ($p \in \mathbb{N}$, $i \in \{A,B\}$) $S$ reaches a ground state, GS. A state is called GS if oscillator $i$ has just fired its $p$th time, and if its phase is zero. We additionally demand that, if the other oscillator's phase $\Phi_j(t_{p,i}) < \tau$, $j$ must have fired at $t_{p,i} - \Phi_j$. This second condition is not necessary in a mathematical sense, but makes the analysis easier by reducing the number of case distinctions. Note that the phase difference in a GS is by definition $\Delta\Phi_{i,j}(t_{p,i}) = \Phi_j(t_{p,i}) - \Phi_i(t_{p,i}) = \Phi_j(t_{p,i}) =: \Phi_{p,i}$. Now, we are able to define a firemap and a return map, similiarly as in [19].

(i) Firemap $h$: $\Phi_{p,i} \rightarrow \Phi_{q,j}$: $\Phi_{q,j} = h(\Phi_{p,i})$ with $t_{q,j} = \min_{r \in \mathbb{N}, k \in \{A,B\}}\{t_{r,k} | t_{r,k} > t_{p,i}\}$.

(ii) Return map $R$: $\Phi_{p,i} \rightarrow \Phi_{p+1,i}$: $\Phi_{p+1,i} = R(\Phi_{p,i})$ $R$ maps the phase difference $\Phi_{p,i}$ when $i$ fires onto the phase difference $\Phi_{p+1,i}$ when $i$ fires again.

The dynamics of $S$ does not depend smoothly on the initial phase difference $\Phi := \Phi_{p,i}$ and the coupling strength $\epsilon$, and must therefore be described by sets of different equations. This is due to the nonvanishing delay $\tau$ and the absorption at threshold [$\epsilon > 0$, min condition in Eq. (2)] or at zero level of $f$ [$\epsilon < 0$, max condition in Eq. (3)]. As the main parameters are the initial phase difference $\Phi$ and the coupling strength $\epsilon$, our strategy is to divide the ($\Phi, \epsilon$) phase space into disjunct domains, which we treat separately, leading to a single explicit form of $h$ in each of them. In the final analysis, these firemaps $h$ have to be combined together to determine the long-term behavior of $S$.

Before we begin the analysis of the different cases or configurations of the dynamics, we want to illustrate our motivation for our choice of intervals in the subspace of initial phase differences $\Phi$. Let us consider that $S$ is a GS with oscillator $A$ just being reset to $\Phi_A = 0$ such that $\Phi = \Phi_B$. In a first interval $I1$, both oscillators have fired, but their spikes did not reach their destination yet. Therefore, the consequences of the two pulses being received have to be evaluated. In a second interval $I2$, only the spike of oscillator $A$ did not reach $B$ and has to be taken into account. In a third interval $I3$, oscillator $B$ will reach the threshold before the

spike of $A$ can be received. These considerations lead to the following definitions for $I1$, $I2$, and $I3$:

$$I1: \quad \Phi_{k,i} \in [0,\tau[,$$

$$I2: \quad \Phi_{k,i} \in [\tau, 1-\tau],$$

$$I3: \quad (\text{Ex0,In0}): \quad \Phi_{k,i} \in \ ]1-\tau, 1].$$

On the one hand, the dynamics is very simple if we are looking at domain $I3$. After a time $t = 1 - \Phi$ (from here on, we identify $t$ with the time elapsed since $S$ has been in a GS), $S$ will be in a GS with $\Phi_B = 0$, which leads to a firemap $h(\Phi) = 1 - \Phi$. Additional case distinctions are not required here, and $I3$ will be referenced as region Ex0 (for excitatory couplings) or In0 (for inhibitory couplings) for reasons of conformity.

On the other hand, the detailed analysis of $I1$ and $I2$ following in the next section requires one to distinguish between excitatory and inhibitory coupling. In each case, we first heuristically describe the temporal development of $S$ to motivate the mathematical notation of the dynamics that will follow afterwards. For brevity, we denote a spike originating from oscillator $A$ as ''spike $A$'' and the oscillator $A$ simply as ''$A$.'' Each domain will be partitioned into smaller regions, which we denote Ex$n$ or In$n$ with successive numbering for excitatory and inhibitory coupling, respectively.

### A. Excitatory couplings, $\epsilon > 0$

#### 1. Configuration I1

At $t = \tau - \Phi$, spike $B$ reaches $A$, and later at $t = \tau$, spike $A$ reaches $B$. Four cases must be distinguished. If $\epsilon$ is very high, $A$ crosses threshold immediately (Ex4) while receiving the spike of $B$. If $\epsilon$ is still high enough, $A$ reaches threshold not immediately, but before spike $A$ can arrive at $B$ (Ex3). Intermediate values of $\epsilon$ only cause spike $A$ to raise $B$ instantaneously above threshold (Ex2). Low values of $\epsilon$ cannot bring either of the oscillators up to fire immediately after absorbing a spike (Ex1). Because the case distinctions necessary for a complete analysis of the time evolution of the system are quite complicated, we use in the following consistently a tabular form where the relevant time steps are shown together with corresponding phases of the oscillators. The motivation or justification for the upper limits of $\epsilon$ can be found in the lines that are marked with an asterisk.

Ex1: $\epsilon < 1 - f(\Phi + \tau)$ and $\Phi \in$ $I1$:

| time $t$ | $\Phi_A$ | $\Phi_B$ |
|---|---|---|
| 0 | 0 | $\Phi$ |
| $\tau - \Phi$ | $\tau - \Phi \rightarrow$ | $\tau$ |
|  | $F_+(\tau - \Phi, \epsilon)$ |  |
| $\tau$ | $F_+(\tau - \Phi, \epsilon) + \phi$ | $\tau + \phi \rightarrow$ |
|  |  | $F_+(\tau + \Phi, \epsilon) < 1$ (*) |

$$h(\Phi) = 1 - [F_+(\tau + \Phi, \epsilon) - (F_+(\tau - \Phi, \epsilon) + \Phi)]. \quad (5)$$

Since $\Phi_A(\tau) \geqslant \tau$ and $\Phi_B(\tau) < 1$, $h(\Phi) > 1 - 1 + \tau + \Phi \geqslant \tau$ such that $h$: Ex1 $\mapsto I2 \cup I3$. Additionally, the phase difference $\Delta\Phi_{A,B}$ increases because the phase shift $\Delta\Phi_B$ is larger than the phase shift $\Delta\Phi_A$.

Ex2: $1 - f(\Phi + \tau) \leqslant \epsilon < f(1 - \Phi) - f(\tau - \Phi)$ and $\Phi \in I1$:

| time $t$ | $\Phi_A$ | $\Phi_B$ |
|---|---|---|
| 0 | 0 | $\Phi$ |
| $\tau - \Phi$ | $\tau - \Phi \rightarrow$ | $\tau$ |
|  | $F_+(\tau - \Phi, \epsilon)$ |  |
| $\tau$ | $F_+(\tau - \Phi, \epsilon) + \Phi$ (*) | $\tau + \Phi \rightarrow$ |
|  |  | $F_+(\tau + \Phi, \epsilon) = 1$ |

$$h(\Phi) = 1 - [1 - (F_+(\tau - \Phi, \epsilon) + \Phi)] = F_+(\tau - \Phi, \epsilon) + \Phi. \quad (6)$$

$h$ will be $h(\Phi) > \tau - \Phi + \Phi = \tau$ such that $h$: Ex1 $\mapsto I2 \cup I3$.

Ex3: $f(1 - \Phi) - f(\tau - \Phi) \leqslant \epsilon < 1 - f(\tau - \Phi)$ and $\Phi \in I1$:

| time $t$ | $\Phi_A$ | $\Phi_B$ |
|---|---|---|
| 0 | 0 | $\Phi$ |
| $\tau - \Phi$ | $\tau - \Phi \rightarrow$ | $\tau$ |
|  | $F_+(\tau - \Phi, \epsilon) < 1$ (*) |  |
| $\tau - \Phi +$ | $1 \rightarrow 0$ | $\tau +$ |
| $[1 - F_+(\tau - \Phi, \epsilon)]$ |  | $[1 - F_+(\tau - \Phi, \epsilon)]$ |
| $\tau$ | $\Phi - 1 +$ | $\tau + \Phi \rightarrow$ |
|  | $F_+(\tau - \Phi, \epsilon)$ | $F_+(\tau + \Phi, \epsilon) = 1$ |

$$h(\Phi) = \Phi - [1 - F_+(\tau - \Phi, \epsilon)]. \quad (7)$$

Since $1 - F_+(\tau - \Phi, \epsilon) > 0$ (*), $h(\Phi) < \Phi$. This assures that $h$: $I1 \mapsto I1$. More precisely, $h$: Ex3 $\mapsto$ Ex3 $\cup$ Ex4, because the slope of the lower bound of Ex3 is positive (as can easily be seen from $d[f(1 - \Phi) - f(\tau - \Phi)]/d\Phi = -f'(x) + f'(y) > 0$ with $x := 1 - \Phi > \tau - \Phi =: y$.) Intuitively, the domains Ex1 and Ex2 cover higher values of $\Phi$ and lower values of $\epsilon$ such that an decrease in phase difference cannot map in those regions.

Ex4: $1 - f(\tau - \Phi) \leqslant \epsilon$ and $\Phi \in I1$:

| time $t$ | $\Phi_A$ | $\Phi_B$ |
|---|---|---|
| 0 | 0 | $\Phi$ |
| $\tau - \Phi$ | $\tau - \Phi \rightarrow$ | $\tau$ |
|  | $F_+(\tau - \Phi, \epsilon) = 1$ |  |
| $\tau$ | $\Phi$ | $\tau + \Phi \rightarrow$ |
|  |  | $F_+(\tau + \Phi, \epsilon) = 1$ |

$$h(\Phi) = \Phi. \quad (8)$$

$h$:Ex4$\mapsto$Ex4 with the same initial conditions but $A$ and $B$ exchanged. Ex4 is a region of marginal stable fixed points.

### 2. Configuration I2

Two cases have to be considered. After $t=\tau$, spike $A$ reaches $B$, which will fire next. Depending on $\epsilon$, $B$ reaches threshold immediately (Ex6) or later (Ex5).

Ex5: $\epsilon < 1 - f(\Phi + \tau)$ and $\Phi \in I2$:

| time $t$ | $\Phi_A$ | $\Phi_B$ |
|---|---|---|
| 0 | 0 | $\Phi$ |
| $\tau$ | $\tau$ | $\Phi + \tau \rightarrow$ |
|  |  | $F_+(\Phi + \tau, \epsilon) < 1$ (*) |

$$h(\Phi) = 1 - \{f^{-1}[f(\tau + \Phi) + \epsilon_+] - \tau\}. \qquad (9)$$

As can easily be seen in Eq. (9), $\tau < h(\Phi) < 1 - \tau$, so $h$:Ex5$\mapsto$I2.

Ex6: $1 - f(\Phi + \tau) \leqslant \epsilon$ and $\Phi \in I2$:

| time $t$ | $\Phi_A$ | $\Phi_B$ |
|---|---|---|
| 0 | 0 | $\Phi$ |
| $\tau$ | $\tau$ | $\Phi + \tau \rightarrow$ |
|  |  | $F_+(\Phi + \tau, \epsilon) = 1$ |

$$h(\Phi) = \tau. \qquad (10)$$

Thus, $h$:Ex6$\mapsto$I2.

### B. Inhibitory couplings, $\epsilon < 0$

#### 1. Configuration I1

$A$ receives spike $B$ at $t = \tau - \Phi$, and $B$ receives spike $A$ at $t = \tau$. Three cases have to be considered: Depending on $\epsilon$, none of the oscillators (In1), one of the oscillators ($B$, In2), or both oscillators ($A$ and $B$, In3) are reset to the resting potential $f = 0$. The mechanism of inhibition induces one more difficulty in our analysis. Due to the fact that the oscillator with higher amplitude $f$ decreases its phase more than the oscillator with lower amplitude while receiving a spike, it is possible that the oscillators exchange their position within the phase axis.

In1: $|\epsilon| \leqslant f(\tau - \Phi)$ and $\Phi \in I1$:

| time $t$ | $\Phi_A$ | $\Phi_B$ |
|---|---|---|
| 0 | 0 | $\Phi$ |
| $\tau - \Phi$ | $\tau - \Phi \rightarrow$ | $\tau$ |
|  | $F_-(\tau - \Phi, \epsilon) > 0$ (*) |  |
| $\tau$ | $F_-(\tau - \Phi, \epsilon) + \Phi$ | $\tau + \Phi \rightarrow$ |
|  |  | $F_-(\Phi + \tau, \epsilon)$ |

$$h(\Phi) = 1 - |\Delta\Phi_{A,B}(\tau)|$$
$$= 1 - |F_-(\tau + \Phi, \epsilon) - F_-(\tau - \Phi, \epsilon) - \Phi|. \qquad (11)$$

We can estimate a lower and an upper bound for $\Delta\Phi_{A,B}(\tau)$ using the monotony of $f$ and relation $A4$, respectively:

$$0 < F_-(\tau + \Phi, \epsilon) - F_-(\tau - \Phi, \epsilon) < 2\Phi \rightarrow |\Delta\Phi_{A,B}(\tau)| < \Phi. \qquad (12)$$

Thus $h$:In1$\mapsto$In0 and $R(\Phi) = h(\Phi)$ if $\Delta\Phi_{A,B}(\tau) < 0$. The phase difference decreases because the absolute value of the negative phase shift $\Delta\Phi_B$ is larger than the phase shift $\Delta\Phi_A$.

In2: $f(\tau - \Phi) < |\epsilon| < f(\tau + \Phi)$ and $\Phi \in I1$:

| time $t$ | $\Phi_A$ | $\Phi_B$ |
|---|---|---|
| 0 | 0 | $\Phi$ |
| $\tau - \Phi$ | $\tau - \Phi \rightarrow$ | $\tau$ |
|  | $F_-(\tau - \Phi, \epsilon) = 0$ |  |
| $\tau$ | $\Phi$ | $\tau + \Phi \rightarrow$ |
|  |  | $F_-(\Phi + \tau, \epsilon) > 0$ (*) |

$$h(\Phi) = 1 - |F_-(\tau + \Phi, \epsilon) - \Phi|. \qquad (13)$$

We can estimate the same lower and upper bounds for $F_-(\tau + \Phi, \epsilon)$ as in In1 using relation $A6$ and the lower bound of $|\epsilon|$:

$$0 < F_-(\tau + \Phi, \epsilon)$$
$$< F_-(\tau + \Phi, f(\tau - \Phi))$$
$$= f^{-1}(f(\tau + \Phi) - f(\tau - \Phi)) \leqslant f^{-1}(f(\Phi + \Phi) - f(\Phi - \Phi))$$
$$\times (A6)$$
$$= 2\Phi. \qquad (14)$$

Thus $h$:In1$\mapsto$In0 and $R(\Phi) = h(\Phi)$ if $\Delta\Phi_{A,B}(\tau) < 0$.

In3: $f(\tau + \Phi) \leqslant |\epsilon|$ and $\Phi \in I1$:

| time $t$ | $\Phi_A$ | $\Phi_B$ |
|---|---|---|
| 0 | 0 | $\Phi$ |
| $\tau - \Phi$ | $\tau - \Phi \rightarrow$ | $\tau$ |
|  | $F_-(\tau - \Phi, \epsilon) = 0$ |  |
| $\tau$ | $\Phi$ | $\tau + \Phi \rightarrow$ |
|  |  | $F_-(\Phi + \tau, \epsilon) = 0$ |

$$h(\Phi) = R(\Phi) = 1 - \Phi. \qquad (15)$$

Thus $h$:In1$\mapsto$In0.

#### 2. Configuration I2

Three cases have to be considered. At $t = \tau$, spike $A$ reaches $B$. Depending on $\epsilon$, $B$ is reset to the resting potential (In6) or not (In4, In5). The difference between In4 and In5 will be clarified in Appendix B.

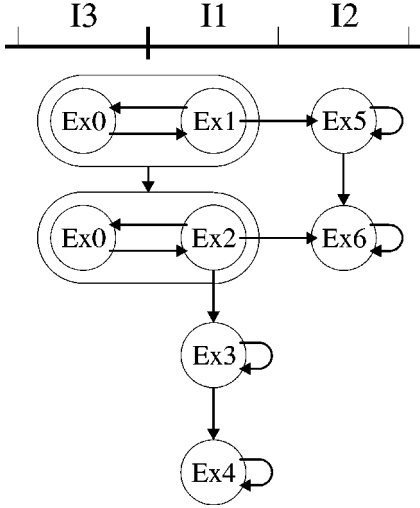In4: $|\epsilon| < f(\tau + \Phi) - f(2\tau)$ and $\Phi \in I2$:

FIG. 2. The flow of the dynamics for excitatory couplings. Initializations in $I2$ terminate in Ex6 (synchronization with phase lag $\tau$), whereas initializations in $I3$ or $I1$ terminate either in $I2$, in Ex4 (marginal stable synchronization with phase lag smaller than $\tau$), or remain in (Ex0-Ex2) if the fixed point in this loop is stable (see text).

| time $t$ | $\Phi_A$ | $\Phi_B$ |
|---|---|---|
| 0 | 0 | $\Phi$ |
| $\tau$ | $\tau$ | $\tau+\Phi\rightarrow$ |
| | | $F_-(\Phi+\tau,\epsilon)>0$ (*) |

$$h(\Phi)=1-\{f^{-1}[f(\tau+\Phi)-|\epsilon|]-\tau\}. \qquad (16)$$

The consequences of this firemap are discussed in Appendix B, too.

In5: $f(\tau+\Phi)-f(2\tau)\leq|\epsilon|<f(\tau+\Phi)$ and $\Phi\in I2$:
Same dynamics table as in $I2$, In4,

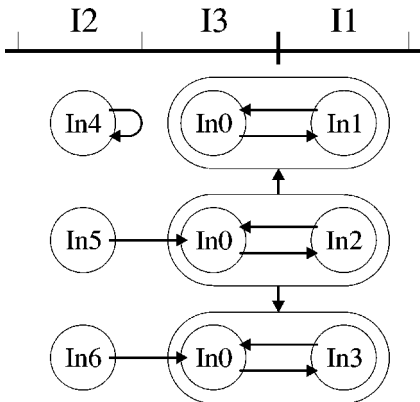$$h(\Phi)=1-|F_-(\tau+\Phi,\epsilon)-\tau|. \qquad (17)$$



FIG. 3. The flow of the dynamics for inhibitory couplings. Initializations in In4 map onto In4 (antiphase synchronization), whereas initializations in any other region terminate either in (In0-In1) if $\epsilon\leq 1-f(\tau)$ (arrow up, in-phase synchronization) or in (In0-In3) if $\epsilon>1-f(\tau)$ (arrow down, synchronization with a phase lag up to $\tau$).

Since $0<F_-(\tau+\Phi,\epsilon)\leq F_-(2\tau,\epsilon=0)=2\tau$, $|F_-(\tau+\Phi,\epsilon)-\tau|<\tau$ such that $h:$In5$\mapsto$In0 and $R(\Phi)=h(\Phi)$ if $\Delta\Phi_{A,B}(\tau)<0$.

In6: $f(\tau+\Phi)\leq|\epsilon|$ and $\Phi\in I2$:

| time $t$ | $\Phi_A$ | $\Phi_B$ |
|---|---|---|
| 0 | 0 | $\Phi$ |
| $\tau$ | $\tau$ | $\tau+\Phi\rightarrow$ |
| | | $F_-(\Phi+\tau,\epsilon)=0$ |

$$R(\Phi)=h(\Phi)=1-\tau. \qquad (18)$$

$h:$In6$\mapsto$In5.

## IV. CONSTRUCTION OF PHASE DIAGRAMS

Taken together, the firemaps for the different domains Ex0-Ex6, In0-In6 form a single description of the dynamics of $S$. This can be represented by flow diagrams shown here (Figs. 2 and 3). In the next paragraphs, we explain how the firemaps work ''together,'' and which attractors or repellors can be found.

Let us start in domain $I2$ with excitatory couplings. The repellor in Ex5* (Appendix A) drives $\Phi$ to the bound of this domain. All initializations out of the Ex5* map onto $\Phi=\tau$ after at most two iterations of $h$ [Appendices A and D, Eq. (10)]. Since $R(\tau)=\tau$ (Appendix D), there exist two stable fixed points in $I2$, the first one being at $\Phi=\tau$ and the second one at $\Phi=h(\tau)$. Under these conditions, the oscillators synchronize with phase lag $\tau$ since the two stable fixed points correspond to each other in the following way such that depending on the initial conditions, either $A$ fires before $B$ or $B$ fires before $A$.

The next domain we discuss is $I1$. Starting in Ex1, $h$ can map to $I2$ or build a loop with Ex0 ($I3$) [Eq. (5)]. Since $h$ in Ex0 ($I3$) does not change the phase difference, while $h$ in Ex1 increases it, the (Ex1-Ex0) loop increases the phase difference. At some time, the phase difference has been grown so much that $h$ maps onto $I2$ or onto Ex2 [if $\epsilon>1-f(2\tau)$]. Depending on the behavior of $S$ in the (Ex2-Ex0) loop (see Appendix C), it is possible that $h$ maps onto $I2$ or Ex3. In Ex3, the phase difference decreases more and more [Eq. (7)] until the domain of marginal stable fixed points Ex4 [Eq. (8)] is reached. An interesting feature of Ex3 and Ex4 is that each oscillator fires twice before the other one can fire again. This can be interpreted such that in one cycle with two spikes of each oscillator, oscillator $A$ is ''leading,'' and in the next cycle, oscillator $B$ is ''leading.'' In Fig. 4, we have plotted an example for $\tau=0.2$. Throughout our illustrations, we use for $f$ the standard example of Mirollo and Strogatz [19] with $b=3$:

$$f(\Phi)=\frac{1}{b}\ln\{1+[\exp(b)-1]\Phi\}, \qquad (19)$$

which yields a particularly simple piecewise linear return map.

Next, we consider inhibitory couplings where we also start with the discussion of $I2$. It can easily be seen that no
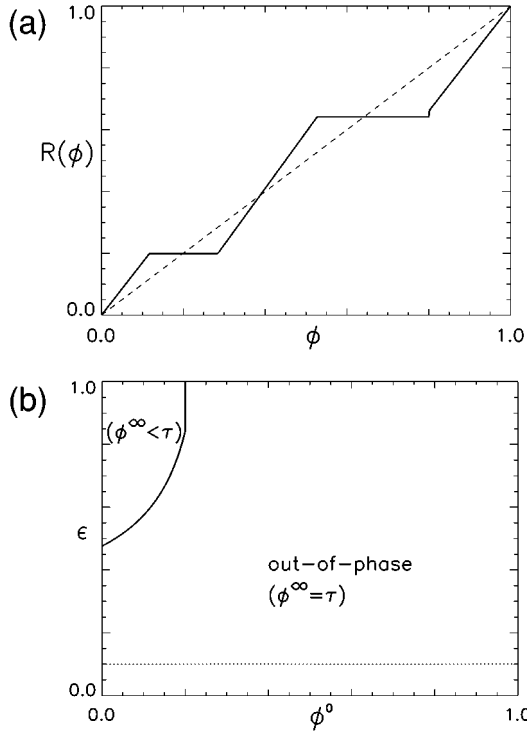
FIG. 4. (a) Return map $R$ for excitatory coupling of strength $\epsilon = 0.1$ with delay $\tau = 0.2$ in the Mirollo-Strogatz model. Two stable fixed points lead to asymptotic out-of-phase synchronization with phase difference $\Phi^\infty = \tau$. (b) Phase diagram determining the asymptotic behavior in dependence of the coupling strength $\epsilon$ and the initial phase difference $\Phi^0$. Out-of-phase synchronization with phase lag $\tau$ is stable everywhere apart from the upper left corner where synchronization with phase lag smaller than the delay is possible. The dashed line denotes the parameter value $\epsilon$ of the particular return map shown in (a).
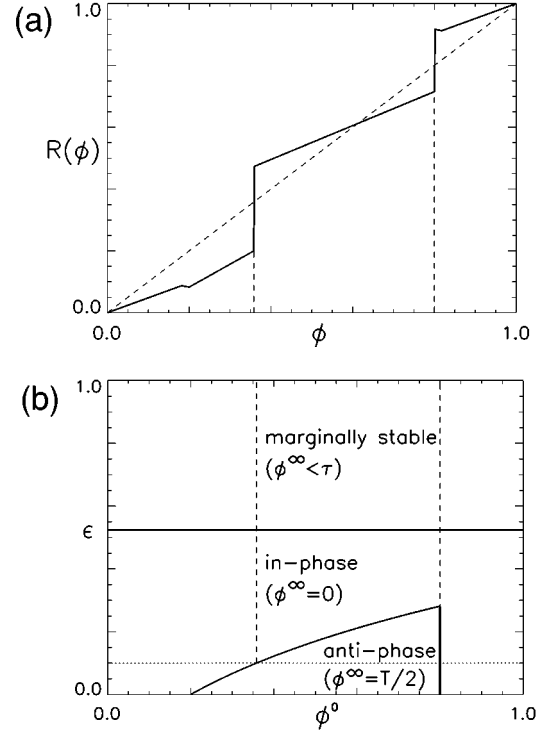


FIG. 5. (a) The return map $R$ for inhibitory coupling with $\epsilon = 0.1$ and $\tau = 0.2$ shows two stable fixed points giving rise to in-phase ($\Phi^\infty = 0$) or antiphase ($\Phi^\infty = T/2$) synchronization. The respective basins of attraction determine the phase diagram (b) as indicated by the dashed lines for their particular value of $\epsilon$ under consideration. For intermediate values of $\epsilon$, the oscillators always fire simultaneously. Large $\epsilon$ leads to marginally stable synchronization with phase lag $\Phi^\infty \leqslant \tau$.

domain maps onto In4 but itself [Eqs. (12)–(18)]. In In4 we find an attractive fixed point (see Appendix B) that synchronizes the oscillators in antiphase. Initializations in In5 and In6 are mapped by $h$ onto In0 ($I3$) [Eqs. (17) and (18)]. The domain In0 ($I3$) itself builds several loops with In1-In3 ($I1$) [Eqs. (11)–(15)]. From Eq. (14) we see that the phase difference decreases in the (In2-In0) loop. At some time the phase difference will be so small that if $\epsilon < 1 - f(\tau)$, $h$ maps onto In1, and if $\epsilon \geqslant 1 - f(\tau)$, $h$ maps onto In3. Under the (In1-In0) loop, the phase difference decreases [Eq. (12) until the oscillators will fire simultaneously; under the (In3-In0) loop, a domain of marginal stable fixed points is reached, Eq. (15)] and the phase difference does not change anymore (Fig. 5).

To summarize our analysis, the general behavior of $S$ can be described as follows. With excitatory couplings, the oscillators synchronize with phase lag $\tau$ such that they are not able to fire in unison. Inhibitory couplings lead to either in-phase or antiphase synchronization depending on the initial conditions, if the coupling strength is intermediate. If the coupling is strong, only in-phase synchronization proves stable. Additionally, marginal stable regimes are found, but only for extremely high parameter values. An other mathematical approach [15,16] shows that these results also apply for integrate-and-fire neurons coupled via $\alpha$ functions.

## V. $N \geqslant 2$ NEURONS

The evaluation of return maps for more than two neurons requires an increasing number of case distinctions and is difficult to manage even if $N > 2$ is small. Therefore we performed computer simulations to uncover the dynamics of the system.

In this section, we present simulations of $N = 100$ neurons with phases $\Phi_i, i = 1, \ldots, N$, either inhibitorily or excitatorily coupled with delay $\tau < 0.5$ and initialized with a uniform random distribution of initial phases.

We find that with both inhibitory and excitatory couplings, the neurons tend to cluster their activities. After a few firing periods, the oscillators split in $N_c$ groups or clusters, where all of the neurons within the same cluster are synchronized with phase lag $\Delta\Phi = 0$. The groups themselves fire alternately, thus leading to a frequency in the summed network activity that is $N_c$ times higher than the individual oscillator frequency. A noise level of $\eta$ is simulated by modifying each phase shift $\Delta\Phi_i$ according to $\Delta\Phi_i \to \Delta\Phi_i(1 + \eta_i)$, where $\eta_i$ is taken from a Gaussian distribution with mean 0 and standard deviation $\eta$. Taking existence of noise into account, we can clearly see an important difference between excitatory and inhibitory couplings [compare Fig. 6(a) with Figs. 7(a)–7(d)]. While the clusters remain stable with inhibition, the clusters in an excitatory network begin to desynchronize and to disappear simultaneously to the emergence of new clusters. This effect seems to be specific for
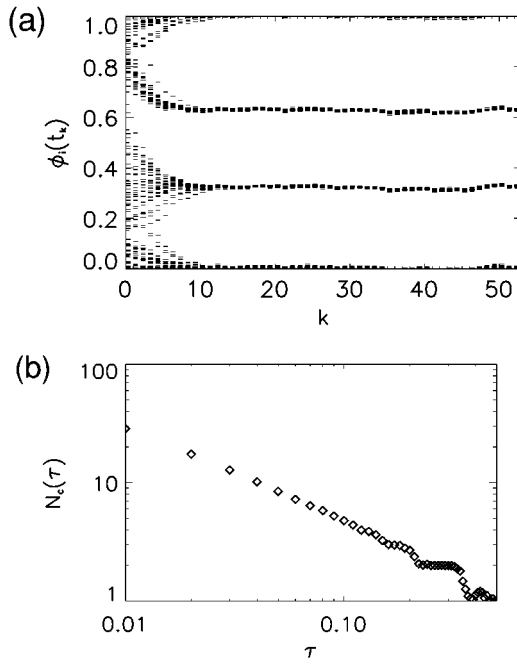
FIG. 6. (a) Stroboscopic view on the phases $\Phi_i(t_k)$ of $N=100$ neurons plotted each time $t_k$ a fixed reference neuron fires its $k$th time. The neurons are inhibitorily coupled with strength $|\epsilon|=0.2$ and delay $\tau=0.2$. The network exhibits multistable clustering and an increase in the network frequency (in this case by about a factor of 3). (b) The average number of stable clusters nearly follows a power law $N_c \sim \tau^{-1}$ as a function of the delay $\tau$ shown here for $\epsilon = 0.2$ and $N = 100$.

pulselike coupling with instantaneous offset. With randomly distributed initial conditions, clusters tend to be of equal size.

Additionally, the clustering with inhibition is multistable. This means that we obtain an arbitrary, but limited number of synchronous clusters only by initializing the oscillators with appropriate phases. As an example, we can evoke one, two, or three subpopulations with fixed network parameters of $N=100$, $\epsilon=-0.1$, and $\tau=0.2$ by choosing $\Phi_i(0)$, $i=1,\ldots,100$, appropriately. In Fig. 6, the maximal number of subpopulations have emerged.

This phenomenon can heuristically be understood by considering the return maps for two neurons. With inhibitory couplings, the fixed point at $\Phi=0$ is stable. All neurons initialized with a phase being within the basin of attraction of this fixed point will be synchronized in one cluster, neurons being outside will be repelled. Another cluster, whose basin of attration also synchronizes all neurons in its neighborhood with zero phase lag, may then emerge in the next interval on the phase axis. This implies that the phase axis is partitioned into intervals of size $\approx 2\tau$, each of them being a basin of attraction for one cluster. Numerous simulations confirmed that this heuristical approach is valid, and we find that the maximum number of clusters roughly follows the power law

$$N_c \approx 1/2\tau \qquad (20)$$

as can be seen in Fig. 6(b).

Considering excitatory couplings, the first fixed point at $\Phi=0$ is a repellor and the second fixed point at $\Phi=\tau$ is an attractor. Imagining two clusters separated from each other by a phase difference of $\tau$, we have two counteracting tendencies. One cluster itself is not stable and is likely to desynchronize, while the other cluster tries to stabilize it. Syn-
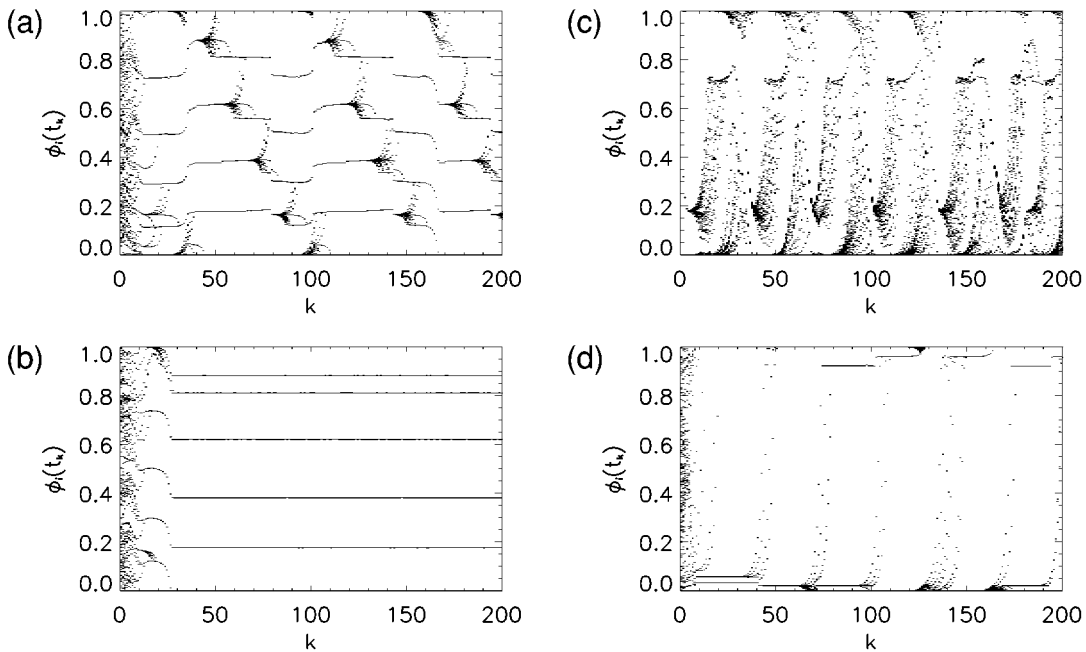


FIG. 7. Stroboscopic views on the phases of $N=100$ excitatorily coupled neurons plotted as in Fig. 6(a) with $\epsilon=0.2$, $\eta=0.0005$, and (a)–(c) $\tau=0.15$, (d) $\tau=0.02$. The network exhibits spontaneous synchronization and desynchronization in various forms. (a) and (b) Two simulations with the same parameters but different random initializations of $\phi_i(0)$ in $[0,1]$. (c) This simulation has been initialized with two synchronous populations in antiphase. (d) Even if the delay and the noise are very small ($\tau=0.02$, $\eta=5\times10^{-9}$), the synchronization becomes unstable.

chronization is only possible if the attractive force overcomes the repulsive one. The balance between these two forces is often unstable, even small amounts of noise can disturb the clustering [Figs. 7(a)–7(d)]. The average number $N_c$ of clusters cannot be expressed as a simple function of the delay $\tau$ [Fig. 10(b)], and it depends sensitively on the initial conditions [Figs. 7(a) and 7(c)].

Very similar phenomena have been observed and analyzed by van Vreeswijk *et al.* [15,16] for networks where the postsynaptic potentials (PSP's) are modeled by $\alpha$ functions. An important parameter in [15,16] is the rise time $\tau_\alpha$ of the $\alpha$ function, which is crucial for the development of synchronicity and clustering. This constant determines the time lag between the onset of the PSP and its maximum amplitude, introducing a *relative* delay similar to the *absolute* delay $\tau$ in our analysis.

We suspect that in real biological systems, clustering depends strongly on the total effective delay $\tau_{\text{eff}}$, which is the sum of the absolute delay $\tau$ and the relative delay $\tau_\alpha \approx 1/\alpha$:

$$\tau_{\text{eff}} = \tau + \tau_\alpha. \tag{21}$$

Evidence for this hypothesis is provided by Figs. 10(c) and 10(d) where we compare simulations with small and large rise times of the postsynaptic potentials, and with varying total delay. By substituting $\tau$ with $\tau_{\text{eff}}$, Eq. (20) is also valid for a ''smooth'' coupling, as can be seen in Fig. 10(d) where all simulations for a wide range of rise times cover the same functional dependency.

## VI. CONTINUOUS DESCRIPTION

In the limit of $N \to \infty$ a network of globally coupled neurons can be described by the dynamics of a probability density function

$$\rho(\phi, t) = \frac{1}{N} \sum_i \delta(\phi - \phi_i(t)) \tag{22}$$

(compare, e.g., [21,16,4,14]). The evolution of the amplitude of one of our model oscillators obeys

$$\frac{df_i}{dt} = v_0 f'(\Phi) + \epsilon \sum_j \delta(t - t_j - \tau), \tag{23}$$

where $t_j, j = 1, \ldots, M$ are the times when the other oscillators emit pulses, and $v_0 = d\Phi/dt$ for $\epsilon = 0$ (compare with Sec. II).

For small individual couplings $\epsilon$ we then have

$$\frac{d\Phi_i}{dt} \approx v_0 + \frac{\epsilon}{f'(\Phi_i)} \sum_j \delta(t - t_j - \tau) \tag{24}$$

from which in the limit of $N \to \infty$ we obtain

$$\frac{d\Phi_i}{dt} = v_0 \left( 1 + \frac{\overline{\epsilon}}{f'(\Phi_i)} \rho(0, t - \tau) \right), \tag{25}$$
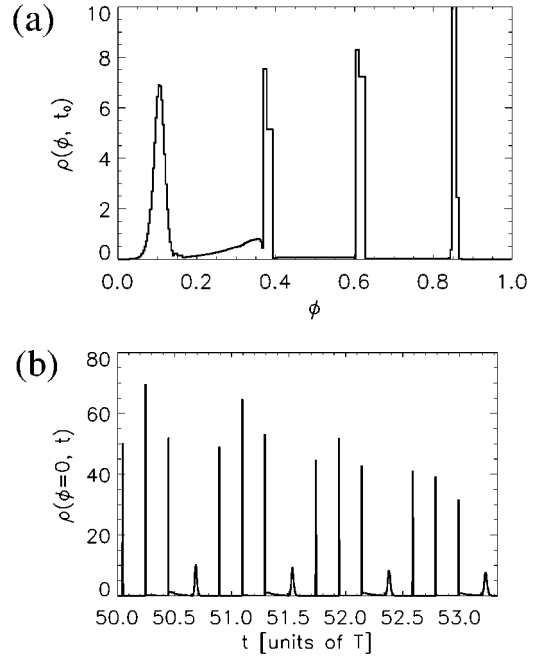


FIG. 8. (a) Snapshot of the continuous model with $\tau = 0.2$ and $\epsilon = 0.2$ at $t_0 = 500T$, where $T := 1/v_0$ denotes the firing period without any coupling. (b) Corresponding time evolution of the instantaneous rate. While synchronized clusters lead to a high population frequency, the offsets of some clusters indicate subsets of asynchronous oscillators.

if we assume that $v(0, t) = v(1, t) = v_0$ (absorption at threshold $\Phi = 0$ or absolute refractoriness at $\Phi = 0$). From this and the boundary condition $\rho(0, t)v(0, t) = \rho(1, t)v(1, t)$ then follows the continuity equation

$$\frac{\partial \rho}{\partial t} = -\frac{\partial(\rho v)}{\partial \phi}, \tag{26}$$

where $v = d\phi/dt$ denotes the drift velocity for $0 < \phi < 1$. Note that the stationary (asynchronous) solution is given by $\rho \propto 1/v$, which in general depends on $\phi$. An analysis of this equation for $\rho(\phi) = 1$ has been presented in [16].

In our simulations, we concentrated on the dependence of the solutions of Eq. (26) on the delay $\tau$. According to the periodic boundary conditions where $v$ is not smooth, we had to simulate Eq. (26) with an algorithm using nonconstant discretization steps.

With inhibitory coupling $\epsilon < 0$, we find an excellent agreement with the multistable clustering seen in Fig. 10(a) (not shown). With excitatory interactions $\epsilon > 0$, we find that the phase density $\rho$ shows a variable number of peaks representing synchronized clusters, although some peaks have a long tail connecting it with its neighbor [Fig. 8(b)]. This side effect of excitation can be related to oscillators that diffuse along the phase axis (not shown). For discrete models, this has also been seen in simulations [22]. Additionally, we find clusters emerging and decaying spontaneously as seen in the discrete dynamics.

## VII. HODGKIN-HUXLEY NEURONS

The description of the well-known Hodgkin-Huxley neuron with its standard parameters can be found in [20]. We

simulated the Hodgkin-Huxley neurons in a globally pulse-coupled network with delay, where the pulses of the neurons were modeled by $\alpha$ functions $E_\alpha(t)$

$$E_\alpha(t) = \begin{cases} \epsilon\alpha^2(t-\tau)\exp[-\alpha(t-\tau)] & \text{for } t > \tau \quad (27) \\ 0 & \text{otherwise.} \quad\quad\quad\quad (28) \end{cases}$$

This realistic model shows a behavior similar to integrate-and-fire neurons. The clustering that is shown in Fig. 9 is multistable and the number of stable clusters increases as the delay decreases (not shown). Due to the relaxation times of the ionic currents in the Hodgkin-Huxley neuron, the effective delay cannot be reduced to $\tau_{\text{eff}} = 0$ such that we were not able to evoke more than three clusters of neurons. These simulations confirmed that this grouping of neurons has to be expected in realistic neuron models and should be relevant for real biological systems as well.

## VIII. DISCUSSION

In this paper, we have analyzed the behavior of two pulse-coupled oscillators in the presence of delays. While delays in oscillatory systems have been the subject of some previous work, this inherent property of most biochemical and physical systems has often been neglected or turned out to be not analytically solvable. The analytical treatment of Mirollo et al. [19] is only valid with excitatory couplings without delay. If some more biological details such as, e.g., an absolute refractory period [23] were added, it becomes questionable if in-phase synchronization can always be achieved.

Our analysis yields two results in this respect. First, we showed that perfect in-phase synchronization is stable only with inhibitory couplings. The corresponding return map has two fixed points leading either to in-phase or antiphase synchronization if the coupling strength $\epsilon$ is intermediate, and to in-phase or marginal out-of-phase synchronization if $\epsilon$ is large. This consequence of inhibitory couplings has already been observed in simulations [24–27,51,52] and analyzed mathematically [16,51] for neurons coupled via pulses of finite width. Conclusively, inhibition may be the best choice to synchronize neurons coupled via substantial delays.

Secondly, excitatory couplings lead to out-of-phase synchronization where the phase lag between the two oscillators is proportional to the delay. These findings extend the work of Mirollo and Strogatz [19], which showed that without delay, in-phase synchronization can be achieved via excitatory couplings. During the course of this work we were informed that a similar, but different analysis [28–30] to ours [31,14] has been carried out yielding qualitatively similar results.

Globally coupled populations of $N > 2$ oscillators show a variety of new phenomena. With excitatory couplings, the oscillators synchronize and desynchronize spontaneously, sensitively depending on the initial conditions such as noise, delay, phases, and coupling strength. Remembering that the fixed point for in-phase synchronization of two neurons is unstable, while the fixed point leading to out-of-phase synchronization is stable, these two counteracting tendencies may be responsible for this interplay between stability and instability.

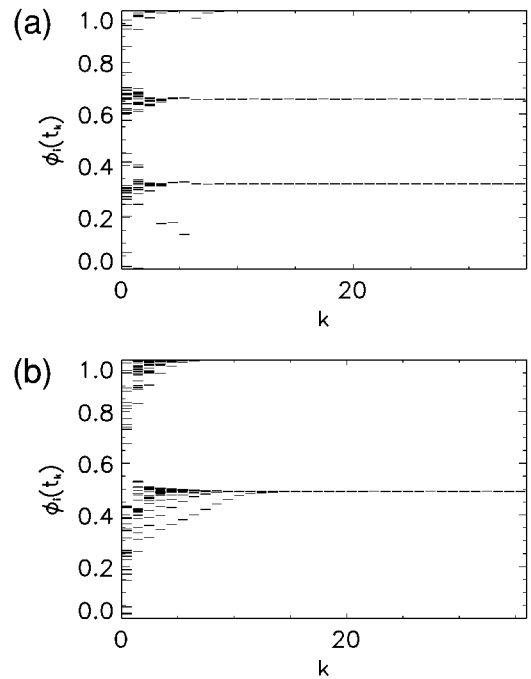Populations coupled with inhibitory weights exhibit mul-



FIG. 9. Stroboscopic views on the phases of $N = 50$ Hodgkin-Huxley neurons with inhibitory coupling plotted as in Fig. 6(a), with (a) $\tau \approx 0$ and (b) $\tau \approx 0.2$. Note that with $\tau \approx 0$, only up to three clusters may emerge due to the "hidden" delays in the ionic conductances.

tistable phase clustering. The oscillators synchronize within several alternately firing groups whose maximal number is determined by the delay time via a power law. The emergence of $N$ clusters leads to a frequency in the summed activity of the network that is $N$ times higher than the individual oscillator frequency. We think that inhibition may be one of the key mechanisms for clustering of neuronal activity in the brain [32,33]. It may also explain the increase in population frequency found in the hippocampus of rats [34], where the network activity exhibits a several times higher frequency than the single neuron.

Nevertheless, the phenomenon of multistable clustering is well known in the literature. Clustering is also possible if the single neuron is not driven continuously and does not oscillate itself [24]. Our results are therefore consistent with previous work, namely, to the stabilization of synchronization by adding inhibitory couplings to an excitatory system [22], and to the emergence of a variety of spatiotemporal patterns [35], but in this framework, they are exclusively the consequences of a *delayed* interaction.

The generalization of the dynamics of $N$ coupled oscillators to arbitrary system sizes by means of a single differential equation for a phase-density function has been the subject of numerous papers [36–40]. We extended this formalism to account for delays using a phase-dependent phase velocity, which we explicitly derived for the Mirollo-Strogatz neuron class (see Fig. 8).

An important condition for this paper was to keep the model as simple as possible to account for various oscillator classes, especially for integrate-and-fire neurons. The ingredients (membrane potential concave down, threshold condition, and pulselike interaction) are typical for constantly driven biological neurons [41]. A similar work that subsumes
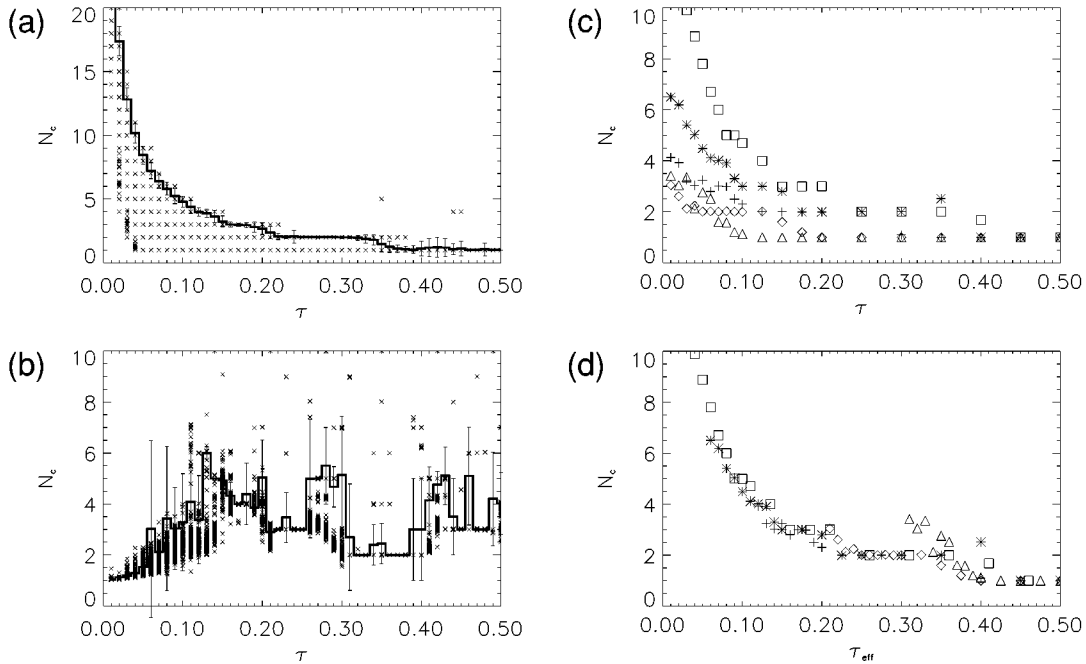
FIG. 10. Dependence of the number of synchronous clusters on the delay of $N = 100$ integrate-and-fire neurons (Mirollo-Strogatz-model) with $b = 0.3$. (a), (b) The bold lines show the average number of clusters $N_c$ emerging from a random initialization, and the crosses show the number of clusters emerging from an initalization of the oscillator's phases in an interval of $[0, \phi_{init}]$. $\phi_{init}$ has been increased from 0.0 to 0.1 in steps of 0.01 and from 0.1 to 1.0 in steps of 0.1. The simulations were performed with an amount of noise equal to a frequency variability of 5%. After the oscillators have been clustered, the noise has been decreased to a finite value in order to see if the oscillators will freeze in a stable configuration. (a) Inhibitory couplings, $\epsilon = -0.2$. (b) Excitatory couplings, $\epsilon = 0.2$. Here, the clustering is not always multistable. (c) Inhibitory couplings, $\epsilon = -0.2$. The pulses were $\alpha$ functions with rise times of 0.01 (boxes), 0.05 (stars), 0.1 (crosses), 0.2 (diamonds), and 0.3 (triangles). (d) shows the same data as in (c) but plotted in dependence of the effective delay $\tau_{eff}$ instead of $\tau$.

different oscillators in a general framework has been done by Gerstner [42], and van Vreeswijk [16]. In the more detailed and somewhat more complex pulse-response model, synchronization can be analyzed analytically [43,44], and has been found if the coupling is inhibitory and delays are of the size of the firing period. If integrate-and-fire neurons are coupled with $\alpha$ functions that introduce a relative delay $\tau_\alpha$, the analysis yields the same results as described in this paper [15,16].

Certainly, other synchronization mechanisms may exist (see, e.g., [45]) and more detailed models may exhibit additional phenomena, but we believe that despite the simplicity of the model we analyzed, the results are typical for neuronal oscillators [16]. We demonstrate this by the model of Hodgkin and Huxley [20] and show that even at this detailed, biological description level, multistable clustering is an emergent property of the network dynamics rather than the result of a nonuniform or learned weight structure [46,43]; and that this phenomenon appears to be quite common in systems where delays are prevalent and inhibitory coupling is strong (Fig. 10).

We believe that the mechanisms proposed in this paper might underlie the synchronization across the two hemispheres of the brain [18] and the synchronous flashing of fireflies [47]. In this respect, it is amazing that the synchronization at species of fireflies having a negative phase shift (''inhibition'') is much more precise than for species using a positive phase shift (''excitation'') [47]. The frequency coupling found in the hippocampus of rats [34] may also indi-

cate that phase clustering plays an important role in real biological networks.

Clustering may be useful for applications where several combinations of stimuli have to be represented at once. Here, multistability is related to the superposition problem [8], and can effectively be used for binding features of different objects simultaneously together. Another application are synfire chains, where the information transported has to be preserved or even sharpened [48]. These topics have already been outlined [49] and will be the subject of our further work [50–52].

## APPENDIX A: FIXED POINT IN Ex5, $\epsilon > 0$

The firemap in domain Ex5 (with $\epsilon \in [0, \epsilon^*[$ and $\epsilon^* := 1 - f(2\tau)$) is given by

$$h(\Phi) := 1 - \{f^{-1}[f(\Phi + \tau) + \epsilon] - \tau\}. \quad (A1)$$

It is easy to check that $h : Ex5 \mapsto I2$ because $\tau < h(\Phi) < 1 - \tau \ \forall (\Phi, \epsilon) \in Ex5$. Let $Ex5^* := \{(\Phi, \epsilon) | h(\Phi) \in Ex5\}$ where we can iterate $h$ twice because $f(\tau + h(\Phi)) + \epsilon < 1$.

We ignore oscillators starting in domain Ex5−Ex5*, which reach the stable fixed point at $\Phi = \tau$ after at most two iterations of $h$. With fixed $\epsilon_0 < \epsilon^*$, Ex5* is given by the open interval

$$\text{Ex5*}|_{\epsilon = \epsilon_0} = ]h^{-1}(\delta), \delta[, \qquad (A2)$$

$$\text{with} \quad \delta = f^{-1}(1 - \epsilon_0) - \tau. \qquad (A3)$$

Starting from $\epsilon_0 < \epsilon^*$, it is easy to prove that this interval is nonempty:

$$\epsilon < 1 - f(2\tau),$$

$$1 + 2\tau - f^{-1}(1 - \epsilon) < 1,$$

$$f(1 + 2\tau - f^{-1}(1 - \epsilon)) < 1,$$

$$f^{-1}[f(1 + 2\tau - f^{-1}(1 - \epsilon)) - \epsilon] - \tau < f^{-1}(1 - \epsilon) - \tau$$

$$h^{-1}(\delta) < \delta, \qquad (A4)$$

Modifying the strategy of [36], we now prove that there exists a unique fixed point of $h$ in Ex5*. First of all, we show the following lemma:

*Lemma 1:* $h'(\Phi) < -1$ and $R'(\Phi) > 1 \quad \forall \Phi \in \text{Ex5*}$.

It suffices to show that $h'(\Phi) < -1$, since $R'(\Phi) = h'(h(\Phi))h'(\Phi)$. From Eq. (A1), we obtain $h'(\Phi) = -f^{-1\prime}[f(\Phi + \tau) + \epsilon]f'(\Phi + \tau)$. Since $f$ and $f^{-1}$ are inverses, the chain rule implies $f'(\Phi + \tau) = \{f^{-1\prime}[f(\Phi + \tau)]\}^{-1}$. Hence

$$h'(\Phi) = -\frac{f^{-1\prime}[f(\Phi + \tau) + \epsilon]}{f^{-1\prime}[f(\Phi + \tau)]}. \qquad (A5)$$

Let $u := f(\Phi + \tau)$. Then Eq. (A5) is of the form

$$h' = -\frac{f^{-1\prime}(u + \epsilon)}{f^{-1\prime}(u)}. \qquad (A6)$$

By hypothesis, $f^{-1\prime\prime} > 0$ and $\epsilon > 0$, so $f^{-1\prime}(u + \epsilon) > f^{-1\prime}(u) \quad \forall u$. Finally, the hypothesis of strict monotonic $f$, thus $f^{-1\prime}(u) > 0$, implies that $h' < -1$, as claimed.

*Proposition 1:* There exists a unique fixed point for $R$ in Ex5*, and it is a repellor.

The fixed point equation for $h$ is $H(\Phi) := \Phi - h(\Phi)$. It is easy to check that $H(\delta) > 0$ and $H(h^{-1}(\delta)) < 0$ [Eq. (A4)]. From Lemma 1 we have $H'(\Phi) = 1 - h'(\Phi) > 0$. Hence $h$, and therefore $R$, have a fixed point $\Phi_0$. Since $R(\Phi_0) = \Phi_0$ and $R'(\Phi) > 1$ by Lemma 1, we have

$$R(\Phi) > \Phi \quad \text{if} \quad \Phi > \Phi_0,$$
$$R(\Phi) < \Phi \quad \text{if} \quad \Phi < \Phi_0. \qquad (A7)$$

Hence the fixed point for $R$ is unique, and is a repellor.

## APPENDIX B: FIXED POINT IN In4, $\epsilon < 0$

The firemap $h$ in In4 is identical to Eq. (A1). The reason for the discrimination between In4 and In5 is that $h : \text{In4} \mapsto \text{In4}$, which we want to check first. Since

$$|\epsilon| < f(\tau + \Phi) - f(2\tau), \qquad (B1)$$

domain In4 is given by $\text{In4}|_{\epsilon = \epsilon_0} = ]a, b[$ with $a := f^{-1}(|\epsilon_0| + f(2\tau)) - \tau$ and $b := 1 - \tau$. First, we show that $h(\Phi) < 1 - \tau = b$:

$$h(\Phi) = 1 - f^{-1}(f(\tau + \Phi) - |\epsilon|) + \tau$$
$$< 1 - f^{-1}(f(2\tau)) + \tau \quad \text{with Eq. (B1)} = b. \quad (B2)$$

Then, we prove that $h(\Phi) > a$.

$$h(\Phi) > 1 - f^{-1}(f(1) - |\epsilon|) + \tau = 1 - f^{-1}(1 - |\epsilon|) + \tau \qquad (B3)$$

Now, we define $\Phi^* := f^{-1}(1 - |\epsilon|)$. With $1 = f^{-1}(f(\Phi^*) + |\epsilon|)$, we write Eq. (B3):

$$h(\Phi) > f^{-1}(f(\Phi^*) + |\epsilon|) - \Phi^* + \tau. \qquad (B4)$$

Since $\Phi^* > 2\tau$, we can write Eq. (B4) using $A7$:

$$h(\Phi) > f^{-1}(f(2\tau) + |\epsilon|) - 2\tau + \tau = a. \qquad (B5)$$

The interval $]a, b[$ is not empty, because $f^{-1}(f(2\tau) + |\epsilon|) < 1$ for all $\epsilon$ within In4.

*Lemma 2:* $0 > h'(\Phi) > -1$ and $R'(\Phi) < 1 \forall \Phi \in \text{In4}$. Lemma 2 can be shown using the same techniques as in Appendix A. The only difference is that the sign of $\epsilon$ is negative.

*Proposition 2:* There exists a unique fixed point for $R$ in In4*, and it is an attractor.

The fixed point equation for $h$ is $H(\Phi) := \Phi - h(\Phi)$. It is easy to check that $H(b) > 0$ and $H(a) < 0$.

$$H(a) = f^{-1}(|\epsilon| + f(2\tau)) - \tau - h[f^{-1}(|\epsilon| + f(2\tau)) - \tau]$$
$$= f^{-1}(|\epsilon| + f(2\tau)) - 1$$
$$< f^{-1}(1) - 1 = 0, \qquad (B6)$$

$$H(b) = 1 - \tau - 1 + f^{-1}(f(1 - \tau + \tau) - |\epsilon|) - \tau = f^{-1}(1 - |\epsilon|)$$
$$- 2\tau > f^{-1}(1 - 1 + f(2\tau)) - 2\tau = 0. \qquad (B7)$$

From Lemma 1 we have $H'(\Phi) = 1 - h'(\Phi) > 0$. Hence $h$, and therefore $R$, have a fixed point $\Phi_0$. Since $R(\Phi_0) = \Phi_0$ and $R'(\Phi) > 1$ by Lemma 1, we have

$$R(\Phi) > \Phi \quad \text{if} \quad \Phi < \Phi_0,$$
$$R(\Phi) < \Phi \quad \text{if} \quad \Phi > \Phi_0. \qquad (B8)$$

Hence the fixed point for $R$ is unique, and is an attractor.

## APPENDIX C: FIXED POINT IN Ex2, $\epsilon > 0$

The only domain where we cannot determine the positions and stability of fixed points whithout explicitly knowing the function $f$ is Ex2. Nevertheless, we prove that fixed points in Ex2 always exist and derive sufficient conditions for their stability.

*Lemma 3:* $\forall \tau \in ]0, 0.5[, \forall \Phi \in ]0, \tau[ \exists \epsilon_F(\tau, \Phi)$ such that $[\epsilon_F(\tau, \Phi), \Phi] \in \text{Ex2}$ and $R(\Phi) = \Phi$.

First of all, we choose

$$\epsilon_F(\tau,\Phi):=f(1-2\Phi)-f(\tau-\Phi). \qquad (C1)$$

Then we have to prove that (a) $[\epsilon_F(\tau,\Phi),\Phi]\in \mathrm{Ex}2$ and (b) $R(\Phi)=\Phi$.

(a) It can easy be seen that

$$\epsilon_F=f(1-2\Phi)-f(\tau-\Phi)>f(1-2\Phi+2\Phi)$$
$$-f(\tau-\Phi+2\Phi) \quad (A5)$$
$$=1-f(\tau+\Phi)=\epsilon_l \qquad (C2)$$

and

$$\epsilon_F=f(1-2\Phi)-f(\tau-\Phi)<f(1-\Phi)-f(\tau-\Phi)=\epsilon_u, \qquad (C3)$$

where $\epsilon_l$ and $\epsilon_u$ denote the lower and upper bounds of Ex2, respectively.

(b) The dynamics starts in Ex2 changing to Ex0 such that $R$ is given by $R(\Phi)=h^{\mathrm{Ex}0}[h^{\mathrm{Ex}2}(\Phi)]$:

$$R(\Phi)=1-h^{\mathrm{Ex}2}(\Phi)=1-F_+(\tau-\Phi,\epsilon_F(\tau,\Phi))-\Phi$$

due to Eq. (16)

$$=1-f^{-1}(f(\tau-\Phi)+f(1-2\Phi)-f(\tau-\Phi))-\Phi$$
$$=1-1+2\Phi-\Phi=\Phi. \qquad (C4)$$

We conclude with a remark on the stability of the fixed points in Ex2. From Eq. (16), it follows that

$$R(\Phi)>\Phi \quad \text{if} \quad \epsilon<\epsilon_F,$$

$$(C5)$$
$$R(\Phi)<\Phi \quad \text{if} \quad \epsilon>\epsilon_F.$$

Obviously, all initializations "above" or "below" the function (C1) lead to a decrement or an increment in the phase difference, respectively:

$$\frac{\partial \epsilon_F(\tau,\Phi)}{\partial \Phi}<0 \quad (\Phi \text{ is an attractor}).$$

$$\frac{\partial \epsilon_F(\tau,\Phi)}{\partial \Phi}>0 \quad (\Phi \text{ is a repellor}). \qquad (C6)$$

### APPENDIX D: $R(\tau)=\tau$ FOR $0<\epsilon\leq 1-F(2\tau)$

It suffices to show that $h(\tau)\mapsto \mathrm{Ex}6$ since $h(\Phi)=\tau \forall \Phi \in \mathrm{Ex}6$. Since $\epsilon<1-f(2\tau)$, the relation $\Phi^*:=f^{-1}(1-\epsilon)>2\tau$ holds true, and it follows from $A7$ that

$$f^{-1}(f(\Phi^*)+\epsilon)-\Phi^*>f^{-1}(f(2\tau)+\epsilon)-2\tau. \qquad (D1)$$

Thus we can estimate a lower bound for $h(\tau)$ using Eq. (D1):

$$h(\tau)=1-f^{-1}(f(2\tau)+\epsilon)+\tau \quad [\text{Eq. (9)}]$$
$$>1+\Phi^*-f^{-1}(f(\Phi^*)+\epsilon)-2\tau+\tau \quad [\text{Eq. (D1)}]$$
$$=f^{-1}(1-\epsilon)-\tau. \qquad (D2)$$

The condition $\epsilon>1-f(\tau+\Phi)$ (lower bound of Ex6) can be transformed into a condition for $\Phi$, $\Phi>f^{-1}(1-\epsilon)-\tau$, which is also true for $h(\tau)$ as can be seen in Eq. (D2). Therefore, $h(\tau)\mapsto \mathrm{Ex}6$.

[1] S. H. Strogatz, C. M. Marcus, R. M. Westervelt, and R. E. Mirollo, Phys. Rev. Lett. **61**, 2380 (1988).

[2] H. Daido, Phys. Rev. Lett. **61**, 231 (1988).

[3] Y. Kuramoto and I. Nishikawa, J. Stat. Phys. **49**, 569 (1987).

[4] Y. Kuramoto, Physica D **50**, 15 (1991).

[5] A. T. Winfree, *The Geometry of Biological Time* (Springer-Verlag, New York, 1980).

[6] C. M. Gray, P. Krönig, A. K. Engel, and W. Singer, Nature (London) **338**, 334 (1989).

[7] R. Eckhorn, R. Bauer, W. Jordan, M. Brosch, W. Kruse, M. Munk, and H. J. Reitboeck, Biol. Cybern. **60**, 121 (1988).

[8] C. v. d. Malsburg, Technical Report No. 81-2, MPI for Biophysical Chemistry, 1981.

[9] C. v. d. Malsburg and W. Schneider, Biol. Cybern. **54**, 29 (1986).

[10] D. Hansel, G. Mato, and C. Meunier, Europhys. Lett. **23**, 367 (1993).

[11] K. Okuda, Physica D **63**, 424 (1993).

[12] D. Hansel, G. Mato, and C. Meunier, Phys. Rev. E **48**, 3470 (1993).

[13] E. R. Grannan, D. Kleinfeld, and H. Sompolinsky, Neural Comput. **5**, 550 (1993).

[14] U. Ernst, K. Pawelzik, and T. Geisel, Phys. Rev. Lett. **74**, 1570 (1995).

[15] C. van Vreeswijk, L.F. Abbott, and G.B. Ermentrout, J. Comp. Neurosci. **1**, 3131 (1994).

[16] C. van Vreeswijk, Phys. Rev. E **54**, 5522 (1996).

[17] W. W. Lytton and T. J. Sejnowski, J. Neurophysiol. **66**, 1059 (1991).

[18] A. K. Engel, P. König, A. K. Kreiter, and W. Singer, Science **252**, 1177 (1991).

[19] R. E. Mirollo and S. H. Strogatz, SIAM (Soc. Ind. Appl. Math.) J. Appl. Math. **50**, 1645 (1990).

[20] A. L. Hodgkin and A. F. Huxley, J. Physiol. (London) **117**, 500 (1952).

[21] L. F. Abbott and C. van Vreeswijk, Phys. Rev. E **48**, 1483 (1993).

[22] M. Tsodyks, I. Mitkov, and H. Sompolinsky, Phys. Rev. Lett. **71**, 1280 (1993).

[23] C.-C. Chen, Phys. Rev. E **49**, 2668 (1994).

[24] C. van Vreeswijk and L. F. Abbott, SIAM (Soc. Ind. Appl. Math.) J. Appl. Math. **53**, 253 (1993).

[25] A. Nischwitz, H. Glünder, A. von Oertzen, and P. Klausner, *ANN Proceedings*, edited by I. Alexander and J. Taylor (Elsevier Science Publishers B.V., Amsterdam, 1992).

[26] M. Tsodyks, I. Mitkov, and H. Sompolinsky, in *Proceedings of the ICANN'93*, edited by S. Gielen and B. Kappen (Springer-Verlag, Berlin, 1993), p. 622.

[27] D. Golomb and J. Rinzel, Phys. Rev. E **48**, 4810 (1993).

[28] L. S. Smith, D. E. Cairns, and A. Nischwitz, in *Proceedings of the ICANN'94*, edited by M. Marinaro and P. G. Morasso

(Springer-Verlag, Berlin, 1994), p. 142.

[29] A. Nischwitz, *Impuls-Synchronisation in Neuronalen Netzwerken* (Verlag Harri Deutsch, Reihe Physik, Thun/Frankfurt, 1994), Vol. 32.

[30] A. Nischwitz and H. Glünder, Biol. Cybern. **73**, 389 (1995).

[31] U. Ernst, K. Pawelzik, and T. Geisel, in *Proceedings of the ICANN'94*, edited by M. Marinaro and P. G. Morasso (Springer-Verlag, Berlin, 1994), p. 916.

[32] X.-J. Wang, D. Golomb, and J. Rinzel, Proc. Natl. Acad. Sci. USA **92**, 5577 (1995).

[33] N. Kopell and G. LeMasson, Proc. Natl. Acad. Sci. USA **91**, 10 586 (1994).

[34] G. Buzsaki, Z. Horvath, R. Urioste, J. Hetke, and K. Wise, Science **256**, 1025 (1992).

[35] W. Wang, G. Perez, and H. A. Cerdeira, Phys. Rev. E **47**, 2893 (1993).

[36] H. U. Bauer and K. Pawelzik, Physica D **69**, 380 (1993).

[37] M. Usher, H. G. Schuster, and E. Niebur, Neural Comput. **5**, 570 (1993).

[38] W. Gerstner and J. L. van Hemmen, Phys. Rev. Lett. **71**, 312 (1993).

[39] L. L. Bonilla, C. J. P. Vicente, and J. M. Rubi, J. Stat. Phys. **70**, 921 (1993).

[40] D. Golomb, D. Hansel, B. Shraiman, and H. Sompolinsky, Phys. Rev. A **45**, 3516 (1992).

[41] L. F. Abbott and T. B. Kepler, in *Statistical Mechanics of Neural Networks*, edited by L. Garrido, Lecture Notes in Physics Vol. 368 (Springer, Berlin, 1990), p. 15.

[42] W. Gerstner, Phys. Rev. E **51**, 738 (1995).

[43] W. Gerstner and J. L. van Hemmen, Network **3**, 139 (1992).

[44] W. Gerstner, Phys. Rev. Lett. **76**, 1755 (1996).

[45] D. Somers and N. Kopell, Biol. Cybern. **68**, 393 (1993).

[46] T. Aoyagi, Phys. Rev. Lett. **74**, 4075 (1995).

[47] J. Buck, Q. Rev. Biol. **3**, 63 (1988).

[48] J. E. Lisman and M. A. P. Idiart, Nature (London) **267**, 1512 (1995).

[49] U. Ernst, K. Pawelzik, and T. Geisel, in *Proceedings of the ICANN'95*, edited by F. Fogelman-Soulié, J.-C. Rault, P. Gallinari, and G. Dreyfus (EC2 & Cie, Paris, 1995), p. 549.

[50] J. Deppisch, H.-U. Bauer, T. Schillen, P. König, K. Pawelzik, and T. Geisel, Network **4**, 243 (1993).

[51] U. Ernst, diploma-thesis, University Frankfurt, 1994 (unpublished).

[52] C. M. Marcus and R. M. Westervelt, Phys. Rev. A **39**, 347 (1989).